Cooling and trapping of ^{85}Rb atoms in the ground hyperfine $F=2$ state

V. B. Tiwari,* S. Singh, H. S. Rawat, and S. C. Mehendale
Laser Physics Applications Division, Raja Ramanna Centre for Advanced Technology, Indore 452013, India
(Received 2 September 2008; published 29 December 2008)

We report cooling and trapping of ^{85}Rb atoms in the lower hyperfine level $F=2$ of the 5 $^2S_{1/2}$ ground state in a magneto-optical trap. A maximum of $\sim 6\times 10^6$ atoms could be trapped using trap laser frequency red detuned by 12 MHz from the $F=2\rightarrow F'=1$ cycling transition. The loading behavior of the trap in terms of loading rate, collisional loss rate, number and density of trapped atoms was studied as a function of trap laser intensity.

DOI: 10.1103/PhysRevA.78.063421 PACS number(s): 37.10.De, 37.10.Gh

The magneto-optical trap (MOT), first demonstrated in 1987 [1] for alkali-metal Na atoms, is the most widely used source of cold neutral atoms. In this trap, three pairs of mutually orthogonal and counterpropagating laser beams and a quadrupole magnetic field are used to cool and trap the atoms simultaneously. In spite of a growing list of atoms from the Periodic Table being successfully cooled and trapped in the MOT, the alkali-metal atoms remain the most widely used source for cold atomic experiments [2]. The ground state of all the alkali-metal atoms have a closed shell with one valance electron resulting in similar energy level structures. The interaction between the nuclear spin I and the electronic angular momentum S for these atoms results in the splitting of the ground state $^2S_{1/2}$ into two hyperfine levels with total angular momentum, $F=I\pm S$. The transition $^2S_{1/2}\rightarrow {}^2P_{3/2}$ (D_2 line) provides a natural choice for trapping these alkali-metal atoms due to its large oscillator strength and availability of cycling hyperfine transitions from the two ground state hyperfine levels. Usually, alkali-metal atom traps have been operated with trapping force provided by cycling transition from the upper hyperfine level of the ground state. However, the difference in specific level separations of each alkali-metal atomic species presents some other interesting trapping conditions as well. For example, trapping of potassium atoms requires the lasers to be red detuned with respect to all hyperfine levels of the excited state [3]. Moreover, various trapping schemes using noncycling transitions from the ground state hyperfine levels of the sodium atom have been investigated. These include trapping of sodium atoms using the $^2S_{1/2}\rightarrow {}^2P_{1/2}$ transition (D_1 line) [4] and type II and III traps [5]. The magnetically induced level-mixing effect of closely placed excited state hyperfine levels corresponding to cycling and noncycling transitions from the lower hyperfine level of the ground state of alkali-metal atoms has been shown to produce confinement of cold atoms [6]. The confinement force and hence the trapped atom population resulting from this effect becomes maximum for zero detuning of the trapping laser from cycling transition. However, an alkali-metal atom trap where the trapping is solely provided by cycling transition from the lower hyperfine level of the ground state has not been reported so far. The difficulty in realizing such a trap can be understood as the following. For hyperfine cycling transition $F\rightarrow F'$ from the lower hyperfine level of the ground state, $F'<F$, and therefore the ground state Zeeman sublevels not coupled to the excited hyperfine level work as dark states as atoms collected in these levels no longer participate in cooling and trapping. Moreover, due to the smaller separation of the excited hyperfine levels, an unavoidable simultaneous partial excitation to the next hyperfine level can decay to the other ground-state hyperfine level.

In this work, we demonstrate magneto-optical trapping of ^{85}Rb atoms where cold atoms are obtained in the ground hyperfine $F=2$ state. The trapping laser was tuned close to the cycling transition $F=2\rightarrow F'=1$, whereas the repumping laser frequency was tuned to the $F=3\rightarrow F'=3$ transition. The loading behavior of this $F=2$ trap in terms of loading rate, collisional loss rate, number and density of trapped atoms was investigated with trap laser intensity. The possibility of trapping an atom using different sets of transitions has been shown to be useful in cold atom collision studies [7] and enhancing the number of trapped atoms for achieving Bose-Einstein condensation [8]. Further, a steady state sample of cold atoms trapped in the lower hyperfine level of the ground state may prove to be useful in quantum optics related experiments [9,10]. Usually, in such experiments, cold atoms in the lower hyperfine level of the ground state are obtained by using the dark MOT technique [11]. However, a requirement of coupling from the upper hyperfine level of the ground state forces the trap to be operated in the transient mode to avoid a likely interference with the cooling and trapping process.

Figure 1(a) shows the schematic of our experimental setup. The MOT uses a vacuum chamber with a pressure of $\sim 2\times 10^{-8}$ torr. Rb vapor is injected in the chamber by passing a constant current of ~ 3.5 A through two Rb-getters fixed in a series. The magnetic field gradient dB/dz at the center of the trap is produced by a pair of quadrupole coils and the stray magnetic fields are removed by the use of three orthogonal pairs of compensating coils. Three orthogonal pairs of σ^+ and σ^- laser beams which are counterpropagating intersect inside the chamber and act as trapping laser beams (T). Two of these pairs of laser beams are inclined at 45° with respect to the vertical z axis and are located in the symmetry plane (yz plane) of the quadrupole coils whereas a third pair of the laser beam is aligned along the axis of the coils (x axis). To prevent optical pumping into the upper

*vbtiwari@rrcat.gov.in

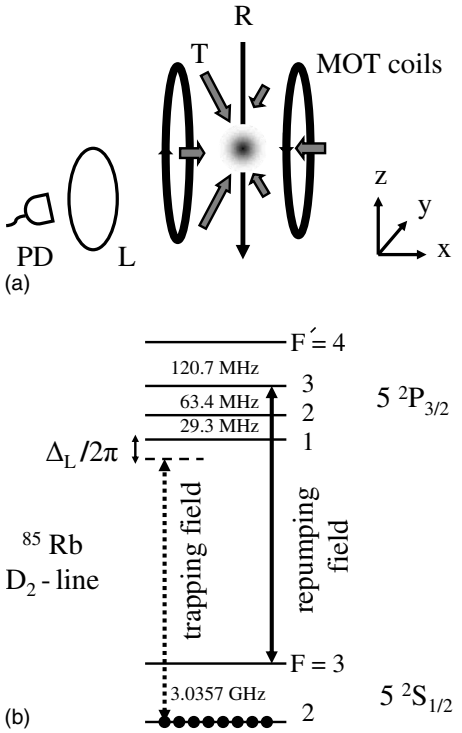

FIG. 1. (a) Schematic of our experimental setup. T: MOT trapping laser beams; R: repumping beam; PD: photodiode; L: collecting lense. (b) The relevant energy levels of ^{85}Rb. See the text for details.

ground-state hyperfine level, a π-polarized repumping laser beam (R) of power 3 mW is separately aligned through the MOT along the vertical z axis. The laser beams are nearly Gaussian with a $1/e^2$ diameter of 7.6 mm. Figure 1(b) shows the energy levels involved in realizing the MOT with ^{85}Rb atoms in $F=2$ state. The trapping laser was locked at the center of the cycling transition $5\ ^2S_{1/2}\ (F=2) \rightarrow 5\ ^2P_{3/2}\ (F'=1)$ of ^{85}Rb atom using the bipolarization spectroscopy (BPS) technique [12] at $\lambda=780$ nm. The BPS technique provides a large dispersive locking signal corresponding to the cycling cooling transition. The natural linewidth of the cooling transition is $\gamma_n=2\pi\times 5.9$ MHz. The red detuning Δ_L from the transition line center is obtained by using a pair of acousto-optical modulators. The repumping laser beam was frequency locked to the peak of $5\ ^2S_{1/2}(F=3) \rightarrow 5\ ^2P_{3/2}(F'=3)$ transition. The frequency locking was done using a Doppler free dichroic lock (DFDL) dispersive signal [13] with relatively large amplitude for the noncycling repumping transition. We observed that the $F=2$ trap works well only when the repumping and trapping beams are well aligned along with stable performance of laser frequency locking. The fluorescence from the atoms loading in the trap was collected on a low noise level photodiode. A weak probe beam of power 1 μW with nearly uniform intensity was passed through the atom cloud for absorption measurements. The probe absorption and fluorescence measurements were independently used to estimate the number and density of the trapped atoms. The spatial profile of the atom cloud was obtained by a digital charge-coupled device camera. The images of expanding atom clouds using this camera also allowed us to determine the temperature. Figure 2(a) shows the image of the ^{85}Rb atom cloud in the $F=2$ trap. The background fluorescence seen along the z axis was due to the repumping beam. Figures 2(b) and 2(c) show the image profiles of the cold atom cloud along the axial and radial directions, respectively, after subtracting the background contribution. These profiles were fitted with Gaussian distributions to obtain the trap volume. The transmission spectra due to the weak probe beam passing through this cold atom cloud is shown in Fig. 3. In this spectra, the $F=2-F'=1,2,3$ curve is

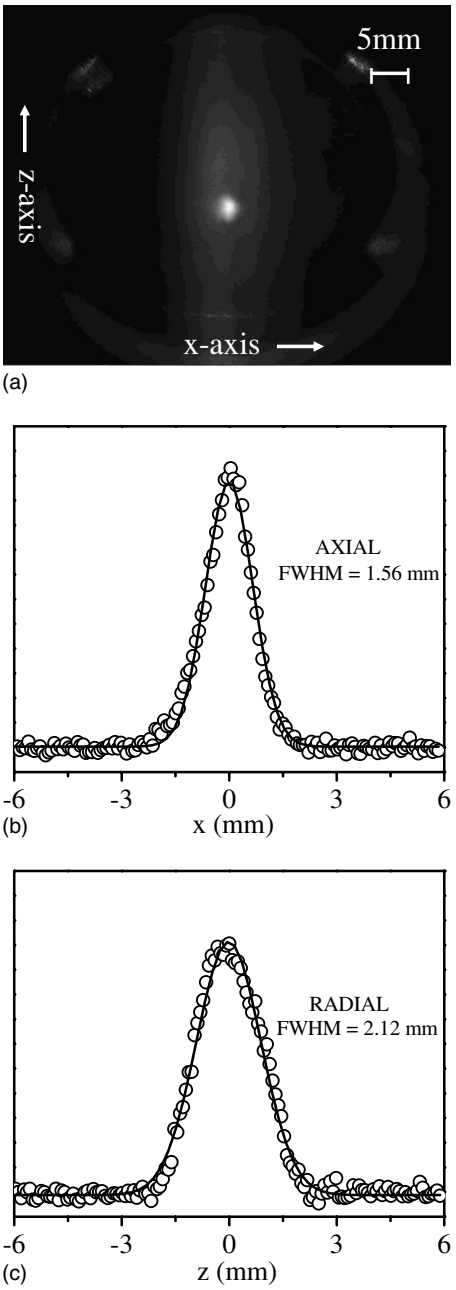

FIG. 2. (a) Image of ^{85}Rb atom cloud in the $F=2$ trap. The background fluorescence along the z axis is due to the repumping beam. (b) Trap profile along the axial direction with subtraction of background. (c) Trap profile along the radial direction with subtraction of background. The solid lines are Gaussian fits to the trap profile.

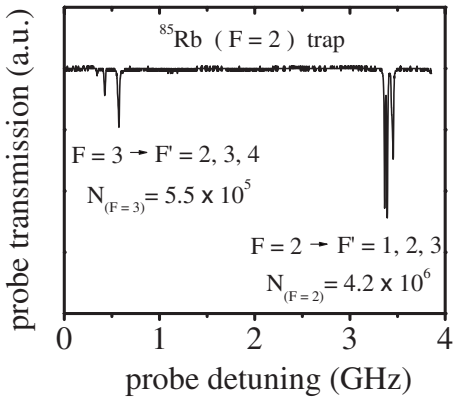

FIG. 3. Transmission spectra for the $F=2-F'=1,2,3$ transitions and $F=3-F'=2,3,4$ transitions for the ^{85}Rb $F=2$ trap. The spectra are recorded for $\Delta_L/2\pi=-12$ MHz, $dB/dz=10$ G/cm, and $s_0=3$.

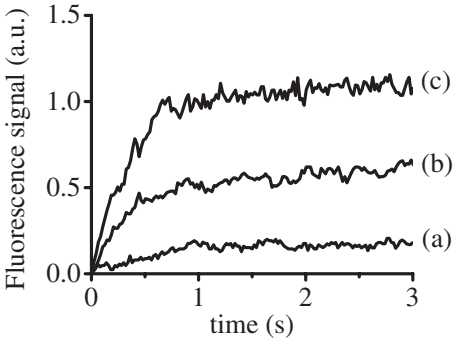

FIG. 4. Trap fluorescence from the ^{85}Rb $F=2$ trap, as a function of time for three values of single trap beam saturation intensity parameter s_0; (a) $s_0=1$, (b) $s_0=3$, (c) $s_0=5$. These curves are obtained for $\Delta_L/2\pi=-12$ MHz, $dB/dz=10$ G/cm, and trap laser beam size ($1/e^2$ diameter) of 7.6 mm.

much more pronounced than the $F=3-F'=2,3,4$ curve, indicating that most of the atoms ($\sim 90\%$) populate the $F=2$ level. The number of trapped atoms estimated by fluorescence and absorption measurements were in good agreement. Further, we studied the loading of atoms in the ^{85}Rb $F=2$ trap. The rate equation governing the number N of trapped atoms is given by [14]

$$\frac{dN}{dt} = L - \gamma N - \beta \int n^2(r,t) d^3r, \tag{1}$$

where L is the rate at which the trap is loaded from the low velocity tail of the Maxwellian velocity distribution for the background Rb atoms. The total loss rate has contributions from two types of collision processes. The first one comes from collision of trapped atoms with hot untrapped atoms which occurs at a rate γ per trapped atom. The second contribution comes from the collision of the trapped atoms among themselves. The loss rate at each position in the trap due to this process is given by $\beta n^2(r,t)$. Here β is the rate coefficient for the trap loss due to collisions between trapped atoms and $n(r,t)$ is the trapped atom density distribution. Usually, the density distribution in MOT is either in a constant volume or constant density regime. In the constant volume regime, as the number of atoms increases in the trap, the density increases, but the atom cloud size remains nearly constant. However, in the constant density regime, the radiation trapping effect becomes prominent and the density distribution is approximated to a constant value. The $F=2$ trap for ^{85}Rb atoms clearly worked in the constant volume regime, as we have observed proportional increase in the density with the number of trapped atoms below $\sim 6\times 10^6$. The density distribution of the trapped atom cloud in the constant volume regime can be written as a Gaussian function,

$$n(r,t) = n_0(t) e^{-r_A^2/2\sigma_{nA}^2} e^{-r_R^2/2\sigma_{nR}^2}, \tag{2}$$

where $n_0(t)$ is the peak density and $r=(r_A^2+r_R^2)^{1/2}$ is the distance from the center of the trap and σ_{nA} and σ_{nR} are the rms width of the Gaussian density distribution in axial and radial directions, respectively. The suffix A (R) denotes axial (radial) direction with respect to the direction of the magnetic coil symmetry axis. The trap volume $V_0=(2\pi)^{3/2}\sigma_{nA}^2\sigma_{nR}$ conveniently connects the number of trapped atoms N to the peak density $n_0(t)$ via $N=n_0(t)V_0$. Equation (2) applied into Eq. (1) gives the following trap loading equation:

$$\frac{dN}{dt} = L - \gamma N - \frac{1}{2^{3/2}} \beta n_0(t) N. \tag{3}$$

For the condition $\frac{dN}{dt}=0$, the number of trapped atoms reaches a steady state value $N_s=L/\Gamma_s$. Here, $\Gamma_s=(\gamma + \frac{1}{2^{3/2}}\beta n_s)$ is the total collisional loss rate corresponding to steady state number N_s and steady state peak density n_s of trapped atoms. Figure 4 shows typical experimental loading curves for various trap laser intensities at fixed detuning and magnetic field gradient. The value of the steady state number of trapped atoms N_s was obtained from the trap fluorescence. We assumed that the trap fluorescence attained steady state value when its variation was less than 5% over a loading period of 100 ms. The steady state peak density n_s was obtained as the ratio of steady state number of trapped atoms N_s and trap volume (V_0). The loading rate L was obtained by measuring the gradient of the loading curve in the first 100 ms. The slope of a linear fit to $N(t)=Lt$, around this region of the loading curve, provided the value of loading rate L. The total collisional loss rate was then simply obtained by the relation $\Gamma_s=L/N_s$. The dependence of the number of trapped atoms on the detuning of the trap laser frequency and the magnetic field gradient is shown in Figs. 5(a) and 5(b), respectively. For the magnetic field gradient, $dB/dz=10$ G/cm, and single beam intensity saturation parameter $s_0=3$, the value of the number of trapped atoms equal to 4.2×10^6 was optimized around trap laser detuning of $\Delta_L/2\pi=-12$ MHz. Here, $s_0=$single trap laser beam intensity/I_s, where $I_s=2.8$ mW/cm^2, is the saturation intensity for the cooling transition. The corresponding density and temperature of the atom cloud was measured to be around 2×10^8 and 4.4 mK, respectively. The red detuning of the trap laser required to optimize the number of trapped atoms clearly suggests that the trapping force is provided by the cycling transition similar to the more usual case of trapping

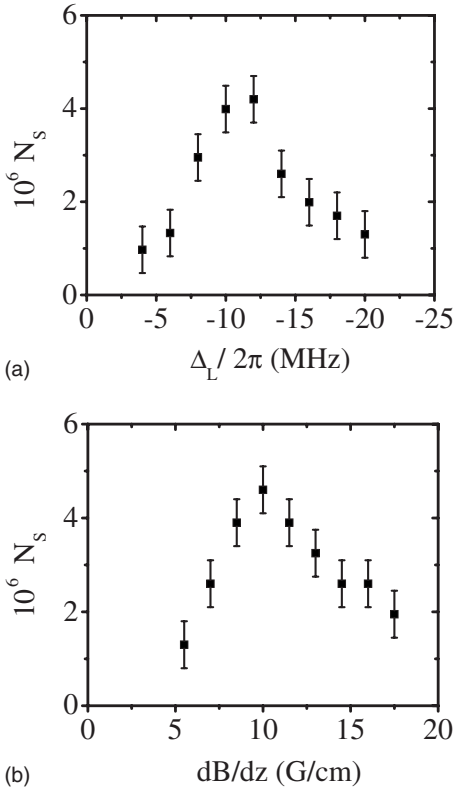

FIG. 5. Steady state number of atoms N_s measured in the ^{85}Rb $F=2$ trap for $s_0=3$, as a function of (a) trap laser detuning $\Delta_L/2\pi$, with respect to the transition $5\,^2S_{1/2}(F=2)\rightarrow 5\,^2P_{3/2}(F'=1)$ with $dB/dz=10$ G/cm, and (b) magnetic field gradient dB/dz, with $\Delta_L/2\pi=-12$ MHz.

using the upper hyperfine level of the ground state.

In Fig. 6, we show how the number of atoms, the density of atoms, the loading rate, and the total collisional loss rate depend on the trap laser intensity. In our experiment with the ^{85}Rb $F=2$ trap, the single trap beam intensity I_{trap} was varied in a range $I_s \leqslant I_{trap} \leqslant 6I_s$, to obtain the steady state number and density of trapped atoms, loading rate, and total collisional loss rate at fixed values of trap laser detuning, magnetic field gradient, and trap beam size. These experimental results were obtained for $\Delta_L/2\pi=-12$ MHz, $dB/dz=10$ G/cm, and trap laser beam size ($1/e^2$ diameter) of 7.6 mm. The nearly linear increase in both number and density of trapped atoms with trap intensity confirms the constant volume regime of MOT operation [Figs. 6(a) and 6(b)]. The total steady state number of trapped atoms N_s initially increases with trap laser intensity and takes a nearly constant value of $\sim 6\times 10^6$ for $s_0=5$. The optimum value of trap intensity for trapping the maximum number of atoms in a MOT is determined by a balance between the loading and loss rates. Figure 6(c) shows the dependence of the loading rate on the trap laser intensity. The loading rate for atoms with velocity less than the capture velocity v_c, is given by $L=n_b V^{2/3} v_c^4/2(2k_B T/m)^3$, where n_b is the density of background Rb atoms, m is the mass of atom, T is the temperature, and V is the capture volume [15]. The trap potential becomes deeper with trap laser intensity, resulting in higher capture velocity v_c for the trap [16]. Therefore the loading

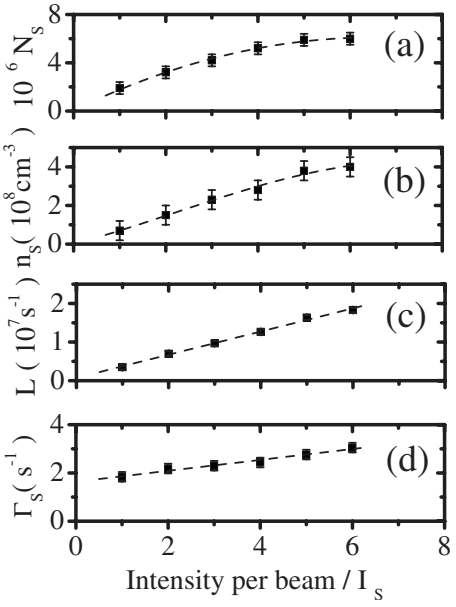

FIG. 6. (a) Steady state number of trapped atoms N_s; (b) steady state density of trapped atoms n_s; (c) loading rate L; (d) total collisional loss rate Γ_s, as functions of the single trap laser beam saturation intensity parameter s_0. The dashed curves are just for visual aid.

rate L increases with trap laser intensity until the saturation effect becomes important. The dependence of total collisional loss rate Γ_s on the trap laser intensity is shown in Fig. 6(d). As discussed earlier, Γ_s is composed of two parts. The first part is in the form of background atom collisional loss rate γ and the other part is the collisional loss rate due to trapped atoms βn_s. To extract these collisional rates from the experimental results, we studied the dependence of the total collisional loss rate Γ_s on steady state density n_s which was varied by changing the trap laser intensity. The results are shown in Fig. 7. The slope of the data provided the collisional loss rate coefficient β. A reasonable linear fit to the data indicates that β is only weakly dependent on trap laser intensity over the range of values studied. The collisions involving excited state atoms increases with trap laser intensi-

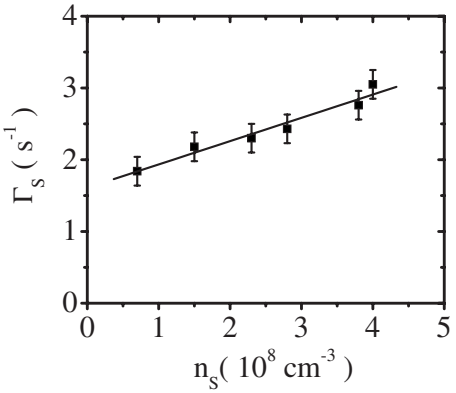

FIG. 7. Dependence of the total collisional loss rate Γ_s on the steady state peak density of trapped atoms n_s for $\Delta_L/2\pi=-12$ MHz, $dB/dz=10$ G/cm, and trap laser beam size ($1/e^2$ diameter) of 7.6 mm. The solid line represents a linear fit.

ties. However, the trap also simultaneously becomes deeper with increase in the trap laser intensity. The near independence of β on trap laser intensity could be due to the competition between these two processes. A similar observation for high values of trap laser intensities in a Rb MOT was obtained by Gensmer *et al.* [17]. Further, the intercept in Fig. 7 gave background atom collisional loss rate γ. We also observed that the intercept varied very little with trap laser intensity, detuning, or magnetic field gradient. It was expected since the process of background atom collisions for constant background pressure is only weakly dependent on the trap depth. Hence from the linear fit to the data in Fig. 7, we found that $\gamma=(1.6\pm0.2)$ s^{-1} and $\beta=(9.1\pm0.7)\times10^{-9}$ cm^3 s^{-1}. The contribution of βn_s towards the total collision loss rate significantly increases for higher values of trap laser intensities, which determines the maximum steady state number of trapped atoms.

In conclusion, we have obtained cold ^{85}Rb atoms using cycling transition involving the ground hyperfine $F=2$ state. The performance of the trap has been investigated in terms of number and density of trapped atoms, loading rate, and total collisional loss rate. The realization of a trap using cycling transition from the lower hyperfine level of the ground state in alkali-metal ^{85}Rb atoms is expected to be useful in studies related to cold atomic collisions, Bose-Einstein condensation, and quantum optics related experiments.

[1] E. L. Raab, M. Prentiss, A. Cable, S. Chu, and D. E. Pritchard, Phys. Rev. Lett. **59**, 2631 (1987).
[2] H. J. Metcalf and P. van der Straten, J. Opt. Soc. Am. B **20**, 887 (2003).
[3] R. S. Williamson III and T. Walker, J. Opt. Soc. Am. B **12**, 1393 (1995).
[4] J. Flemming, A. M. Tuboy, D. M. B. P. Milori, L. G. Marcassa, S. C. Zilio, and V. S. Bagnato, Opt. Commun. **135**, 269 (1997).
[5] S. N. Atutov, V. Biancalana, A. Burchianti, R. Calabrese, S. Gozzini, V. Guidi, P. Lenisa, C. Marinelli, E. Mariotti, L. Moi, K. Nasyrov, and S. Pod'yachev, Eur. Phys. J. D **13**, 71 (2001).
[6] K. Nasyrov, V. Biancalana, A. Burchianti, R. Calabrese, C. Marinelli, E. Mariotti, and L. Moi, Phys. Rev. A **64**, 023412 (2001).
[7] S.-Q. Shang, Z.-T. Lu, and S. J. Freedman, Phys. Rev. A **50**, R4449 (1994).
[8] H. Tanaka, H. Imai, K. Furuta, Y. Kato, S. Tashiro, M. Abe, R. Tajima, and A. Morinaga, Jpn. J. Appl. Phys., Part 2 **46**, L492 (2007).
[9] D. A. Braje, V. Balić, G. Y. Yin, and S. E. Harris, Phys. Rev. A **68**, 041801(R) (2003).
[10] J. Zhang, G. Hernandez, and Y. Zhu, Opt. Lett. **32**, 1317 (2007).
[11] W. Ketterle, K. B. Davis, M. A. Joffe, A. Martin, and D. E. Pritchard, Phys. Rev. Lett. **70**, 2253 (1993).
[12] V. B. Tiwari, S. Singh, S. R. Mishra, H. S. Rawat, and S. C. Mehendale, Opt. Commun. **263**, 249 (2006).
[13] G. Wasik, W. Gawlik, J. Zachorowski, and W. Zawadzki, Appl. Phys. B: Lasers Opt. **75**, 613 (2002).
[14] R. Ejnisman, Y. E. Young, S. B. Weiss, and N. P. Bigelow, Jpn. J. Appl. Phys., Part 1 **38**, 5267 (1999).
[15] C. Monroe, W. Swann, H. Robinson, and C. Wieman, Phys. Rev. Lett. **65**, 1571 (1990).
[16] V. S. Bagnato, L. G. Marcassa, S. G. Miranda, S. R. Muniz, and A. L. de Oliveira, Phys. Rev. A **62**, 013404 (2000).
[17] S. D. Gensemer, V. Sanchez-Villicana, K. Y. N. Tan, T. T. Grove, and P. L. Gould, Phys. Rev. A **56**, 4055 (1997).